

Progressive failure of composite wind blades with a shear-web spar subjected to static testing

T Y Kam* and Y H Chiu

Mechanical Engineering Department, National Chiao Tung University
Hsin Chu 300, Taiwan

*Email: tykam@mail.nctu.edu.tw

Abstract. Composite wind blades of 1m long comprising glass-fabric/epoxy skins and a sandwich plate-type spar were designed and fabricated for static testing. In the composite wind blades, the spar supports the top and bottom skins to form the airfoil shape of NACA4418. The blades were tested to failure and the failure modes were identified at different loading stages. A structural failure analysis method which consists of a geometrically nonlinear finite element (FE) model and appropriate phenomenological failure criteria is used to study the progressive failure behaviours of the blades subjected to different types of quasi-static loads. The experimental load-displacement curves as well as failure loads and locations for different failure modes are used to validate the suitability of the proposed failure analysis method.

1. Introduction

In a wind turbine, the wind blades are used to convert wind energy to electrical power. To attain high efficiency, the structure of a wind blade is required to be light and have small mass moment of inertia so that they can response swiftly to wind direction change and have low cut-in wind speed. During the operating life of a wind turbine, the wind blades have to survive the attack of severe environment. In particular, a wind blade has to be able to sustain the extreme wind loads that may occur during its lifetime. Such load carrying capacity requirement has made the failure analysis of a wind turbine blade become an important topic of research, especially the determination of the failure behaviour of the blade under an extreme wind load. Recently, many papers [1-5] have been devoted to study the failure behaviour of wind turbine blades subjected to quasi-static loads. In the previous studies, the failure modes and their criticality have been studied in the failure analysis of the wind blades. Due to their different structural configurations and loading conditions, large and small composite wind blades may have distinct mechanical behaviours and failure modes. Therefore, to assure the reliability of small wind blades, it is desired to have a deeper understanding about the actual blade failure behaviour. In this paper, the progressive failure behaviour of 1m long composite wind blades comprising a sandwich spar is studied via both experimental and theoretical approaches. The small composite wind blades were subjected to either load- or stroke-control testing. A structural failure analysis procedure is used to analyse the nonlinear failure behaviour of the blades. The experimental results are used to validate the suitability of the proposed failure analysis method.

2. Design and fabrication of composite wind blade

The small composite wind blade shown schematically in Figure 1 consists of 3 main parts, namely, top skin, bottom skin, and longitudinal sandwich spar. The skins are fabricated with glass fabric/epoxy



laminate. The top and bottom skins which are adhesively connected to the spar to form the aerodynamic profile of the blade are adhesively bound to two glass fiber/epoxy stiffeners at, respectively, the leading and trailing edge to prevent delamination or opening failure mode from occurring at these edges. The root end of the blade is also adhesively bound to a rigid metallic connector. The blade orients in the x-direction with its root end located at $x = 0$. Each skin layer has one fiber direction coincident with the span-wise (x) direction and the other with the chord (y) direction. To save weight, the numbers of glass fabric/epoxy layers in the skins vary along the span of the blade. The blade cross section starts to change its shape gradually from airfoil at $x = 0.14\text{m}$ to circle at $x = 0\text{ m}$. The spar is made of two flanges and a shear web. The shear web of the spar is a glass fabric composite sandwich panel and the flanges of the spar are Balsa wood panels. The width and thickness of each spar flange are 30 and 2mm, respectively. For the composite sandwich spar web, each glass fabric face sheet comprises 3 glass fabric/epoxy layers and the core is a 2 mm thick Balsa wood panel. The blade is equally divided into ten stations. The geometric properties such as chord length c , skin thickness t , and twist angle β_T are listed in Table 1. The wind blade has an efficiency of 0.42 for the designed tip speed ratio of 5. The hand layup technique was used to make the parts of the wind blade. Regarding the fabricating process, the moulds used to manufacture the top and bottom blade skins are shown in Figure 2. The glass fabric sheets coated with epoxy resin were placed in the mould and the vacuum forming technique was used to cure the glass fabric/epoxy layers. The parts of the blade including skins, spar, and stiffeners are shown in Figure 3. The assembled wind blade with painted surface is shown in Figure 4. Glass fabric/epoxy panels were also manufactured to determine the material constants of the composite lamina experimentally. The material constants of the glass fabric/epoxy lamina are listed in Table 2.

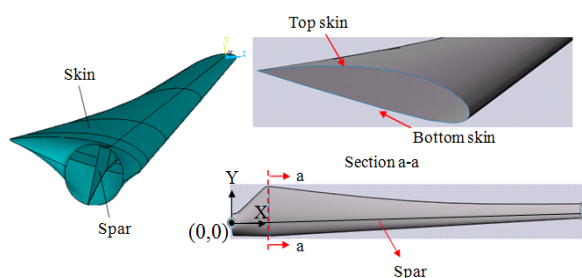


Figure 1. Schematic description of wind blade.



Figure 2. Mould for blade fabrication.



Figure 3. Parts for fabricating wind blade.



Figure 4. Assembled wind blade.

Table 1. Cross-sectional properties of blade at different stations.

Blade length (m)	Property	Twist angle β_T (Degree)	Chord length C (mm)	Skin thickness t (mm) [Layer range (mm)] Number of layers
	Station location (mm)			
1	0	-	-	Top skin 0.75

120	20.00	180.14	[0 \leq X \leq 350] 3 Layers Bottom skin 1.00 [0 \leq X \leq 350] 4 Layer
210	17.01	167.62	
300	13.75	155.76	
390	10.41	144.70	
480	7.26	134.44	0.50 [350 \leq X \leq 1080] 2 Layers
570	4.61	124.84	
660	2.64	115.65	
750	1.30	106.67	
840	0.51	97.78	
930	0.14	88.92	
1020	0.00	80.06	

Table 2. Properties of blade materials.

Material constant	Glass fabric/epoxy	Balsa wood	Strength parameter	Glass fabric/epoxy (MPa)
E_x	20GPa	3.7GPa	X_T	252
E_y	20GPa	55MPa	X_C	305
$G_{xy} = G_{xz}$	2.637GPa	55MPa	Y_T	252
G_{yz}	2.637GPa	8.33MPa	Y_C	305
ν_{xy}	0.15	0.02	S_{xy}	64
ν_{yz}	0.212	0.2	$S_{xz} = S_{yz}$	64

3. Experimental investigation

Several wind blades were subjected to load- and stroke testing for experimental study. In the load-control test as shown in Figure 5, the composite blade with the bottom skin facing upward was fixed at the root end. Several strain gages were mounted on the blade surfaces to measure the blade surface strains during testing. In the double load test, with same increment the total weights of the steel balls in the buckets were increased incrementally. For each blade under load-control testing, when the load was increased to a certain value, the incipient buckling of the front (top) skin of the blade would occur by inducing several dimples on the skin as shown in Figure 6. The location of each dimple was determined by measuring the distance between the dimple center and the blade root. The load that caused the incipient buckling of the blade was identified via the observation of the sign changes of the measured strains. As the load was kept increasing, the failure of blade materials such as skin glass fabric/epoxy lamina (first-ply failure) or adhesive at the interface between skin and spar (skin-spar interfacial debonding) might occur before the total fracture occurs at the blade root. On the other hand, for the blade subjected to stroke-control test as shown in Figure 7, with the front (top) skin facing upward, the blade was fixed at the root end while the blade tip was clamped using a rigid gripper in the form of the blade airfoil shape. The gripper was connected to the MTS material testing machine via a rigid link which consisted of three steel rings in chain. The link with its two ends working as two pin joints, respectively, transmitted an axial force from the testing machine to the blade tip. The

vertical movement of the top end of the link was controlled using the testing machine which was increased incrementally at a speed of 3mm/min. A load cell was used to measure the load associated with the assigned vertical displacement of the link top. The vertical displacements of the link top at different stroke stages together with the associated loads were recorded by a data acquisition system to construct the load-displacement curve. When the blade tip vertical displacement was increased to a certain value, the incipient buckling of the front (top) skin of the blade would occur by inducing a dimple on the skin. The location of the first dimple on the front blade skin and the strains were recorded to determine the incipient buckling load. As the stroke was kept increasing, additional dimples would be developed and a crack would be formed due to the failure of the blade material at the edge of the first dimple as shown in Figure 8. The extension of the crack across the blade skin would finally lead to the total failure of the blade.



Figure 5. Load-control test of wind blade.

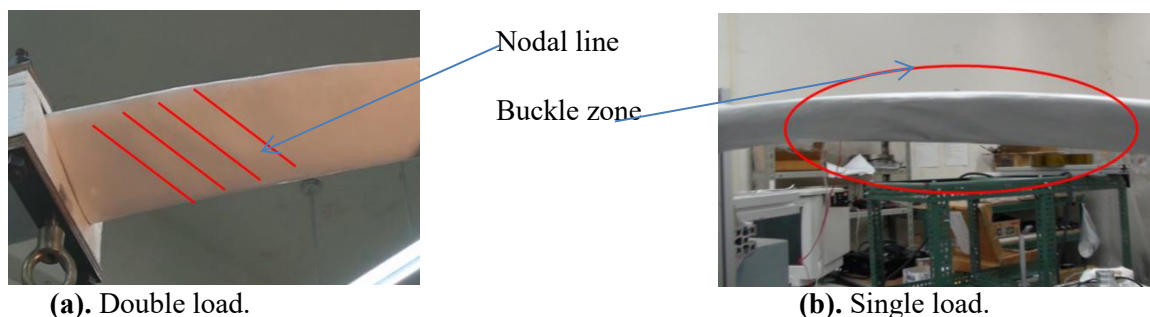


Figure 6. Incipient buckling of blades under load-control testing.

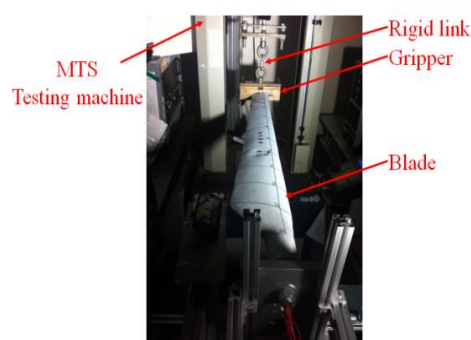


Figure 7. Stroke-control test of blade.

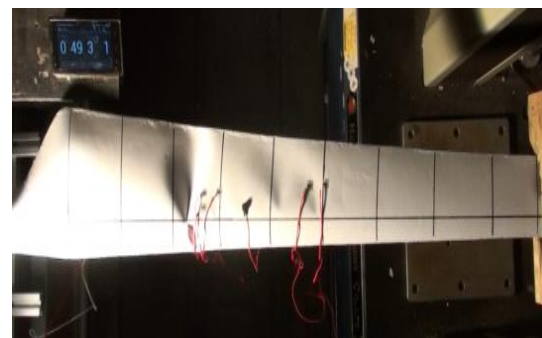


Figure 8. Crack developed from material failure.

4. Experimental and theoretical results

The failure of a small composite wind blade is susceptible to the effects of geometrical nonlinearity. Therefore, in the proposed failure analysis procedure, the geometrically nonlinear FE method of ANSYS [6] together with the Tsai-Wu and quadratic failure criteria for identifying material and interfacial failure, respectively, is used to analyse the failure behaviour of the small composite wind blades which have been tested. In the FE formulation, the composite wind blade is modelled using the laminated composite Shell91 elements of which each has eight nodes and four integration points. To bind the skin and spar together, the nodes of the skin elements are located at the top surfaces of the elements while those of the spar elements at the middle surfaces of the elements. At the critical interfacial regions, a row of thin epoxy elements is used to bind the skin and spar. In the blade failure analysis, the stresses at each layer of an element and the interface between skin and spar are used to determine if material or interfacial failure has occurred. Regarding material degradation due to material failure, the material constants of a lamina in an element are treated as zero when material failure in that lamina is detected to occur. Similarly, when failure occurs in an interfacial element, the material constants of that element become zero. In the nonlinear finite element analysis with the consideration of material degradation, the load-displacement curve is constructed using an incremental displacement procedure in which the tip displacement is increased incrementally via a stroke-control approach. Whenever material failure in the blade is detected, the material constants of the failed element(s) are modified in accordance with the proposed material degradation model and the blade with such new material constants is analysed again starting from the initially undeformed configuration via the incremental displacement approach. The experimental and theoretical load-displacement curves are shown in Figure 9. The experimental results have shown that the bottom skin of the blade buckles at the tip stroke of 66mm (load is 143.9N) with the first dimple at $x = 45\text{mm}$; material failure occurs at $x = 45\text{mm}$, the edge of the first dimple, when the tip stroke is 104mm (load is 212.2N); the applied load drops to 199.4N at the tip stroke of 105mm due to the enlargement of the dimple size; the applied load further drops to 168.9N at the tip stroke of 120mm due to the extension of the crack initiated at the material failure point; the bottom skin is torn apart to make the blade fail totally at the tip stroke of 165mm (load is 59.4N). It is noted that the theoretical load-displacement curve predicted using the material degradation method closely matches the experimental one. The difference between the theoretical and experimental ultimate loads is less than 4%. Therefore, it is appropriate to adopt the proposed material degradation method for progressive failure analysis of small composite wind blade.

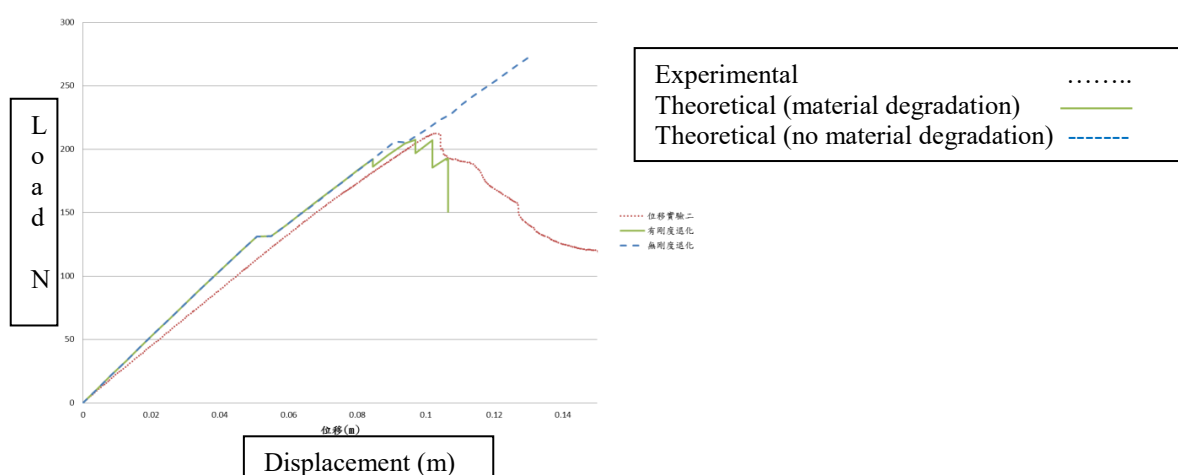


Figure 9. Experimental and theoretical load-displacement curves of blade under stroke-control testing.

5. Conclusion

The progressive failure of small composite wind blade has been studied via both experimental and theoretical approaches. A number of wind blades have been subjected to load- and stroke-control

testing to observe the failure behaviour of the blades. A nonlinear failure analysis method with or without considering material degradation has been proposed. It has been shown that the failure analysis method with the consideration of material degradation is appropriate for progressive failure analysis of small composite wind blades. The difference between the theoretical and experimental ultimate loads is less than 4% for the blade subjected to stroke-control testing.

References

- [1] Overgaard L C T, Lund E and Thomsen O T 2010 Structural collapse of a wind turbine blade Part A: Static test and equivalent single layered models *Composites Part A-Applied Science and Manufacturing* **41** (2) pp 257-70
- [2] Overgaard L C T and Lund E 2010 Structural collapse of a wind turbine blade. Part B: Progressive interlaminar failure models *Composites Part A-Applied Science and Manufacturing* **1** (2) pp 271-83
- [3] Sierra-Perez J, Torres-Arredondo M A and Gueemes A 2016 Damage and nonlinearities detection in wind turbine blades based on strain field pattern recognition. FBGs, OBR and strain gauges comparison *Composite Structures* **135** pp 156-66
- [4] Haselbach P U, Bitsche R D and Branner K 2016 The effect of delaminations on local buckling in wind turbine blades *Renewable Energy* **85** pp 295-305
- [5] Kim S H, Bang H J, Shin H K and Jang M S 2014 Composite Structural Analysis of Flat-Back Shaped Blade for Multi-MW Class Wind Turbine *Applied Composite Materials* **21** pp 525-39
- [6] ANSYS 2010 **12** 1 (ANSYS Inc. USA)

Acknowledgment

This research work was supported by the Ministry of Science and Technology under MOST 105-2221-E-009-149.